

Optical-reflectance anisotropy in epitaxial metastable $(\text{GaAs})_{1-x}(\text{Si}_2)_x(001)$ alloys: A probe for the zinc-blende-to-diamond structural transition

A. Lastras-Martínez and G. Rodriguez-Pedroza

*Instituto de Física, Universidad Autónoma de San Luis Potosí, Alvaro Obregón 64,
San Luis Potosí, San Luis Potosí, Mexico*

D. H. Mei, B. Kramer, D. Lubben, and J. E. Greene

*Department of Materials Science, The Coordinated Science Laboratory, and the Materials Research Laboratory,
University of Illinois, 1101 West Springfield Ave., Urbana, Illinois 61801*

(Received 14 November 1990)

Anisotropy in the above-band-gap optical reflectance along the $[110]$ and $[1\bar{1}0]$ directions has been used to investigate long-range atomic ordering in metastable epitaxial $(\text{GaAs})_{1-x}(\text{Si}_2)_x(001)$ alloys as a function of Si concentration x . The amplitude of the differentiated reflectance-difference signal was found to decrease monotonically with increasing x and reach zero, corresponding to the critical concentration for the zinc-blende-to-diamond transition, at $x \approx 0.37$, consistent with x-ray-diffraction results. The highest sensitivity in the optical-anisotropy spectra was obtained in the spectral region near the E'_0 critical point (4.5 eV in GaAs).

I. INTRODUCTION

Over the past several years, a variety of new epitaxial metastable $(A^{\text{III}}B^{\text{V}})_{1-x}(C_2^{\text{IV}})_x$ alloys including $(\text{GaAs})_{1-x}(\text{Ge}_2)_x$,^{1,2} $(\text{GaSb})_{1-x}(\text{Ge}_2)_x$,³ $(\text{GaSb})_{1-x}(\text{Sn}_2)_x$,⁴ $(\text{GaSb})_{1-x}(\text{Ge}_{2(1-y)}\text{Sn}_{2y})_x$,⁵ and $(\text{GaAs})_{1-x}(\text{Si}_2)_x$ (Ref. 6) have been synthesized from the vapor phase and studies of their optical,^{1,7,8} electrical,⁹ lattice dynamic,^{1,10,11} structural (i.e., atomic ordering),^{2,12,13} and thermodynamic properties^{3,14} reported. A unique feature of these alloys is the requirement of a zinc-blende-to-diamond structural phase transition at some composition intermediate between the III-V and group-IV end members even though short-range order is preserved, i.e., there is no evidence of significant concentrations of $A^{\text{III}}-A^{\text{III}}$ or $B^{\text{V}}-B^{\text{V}}$ bonds.^{10,12} In the case of $(\text{GaSb})_{1-x}(\text{Ge}_2)_x$, the zinc-blende-to-diamond transition has been found by x-ray diffraction to occur at $x \approx 0.3$.¹³

In this paper, we show that a major component of the above-band-gap optical reflectance anisotropy between the $[110]$ and $[1\bar{1}0]$ directions in the zinc-blende lattice is due to preferential surface termination with A^{III} or B^{V} species which, in the presence of well-defined cation and anion sublattices, renders the bonding in the first few monolayers anisotropic. Thus, spectroscopic measurements of the reflectance anisotropy in $(A^{\text{III}}B^{\text{V}})_{1-x}(C_2^{\text{IV}})_x(001)$ alloys can be used to probe long-range ordering. In particular, measurements of the amplitude of the anisotropy spectra from $(\text{GaAs})_{1-x}(\text{Si}_2)_x$ as a function of Si concentration x were used to determine that the zinc-blende-to-diamond transition in this system occurs near $x \approx 0.37$ (i.e., anisotropy is no longer observed at Si concentrations above $x > 0.37$) in agreement with x-ray-diffraction studies. The most sensitive spectral region over the energy range used in

this study, 2.4–5.5 eV, was found to be near the critical point E'_0 .

II. EXPERIMENTAL PROCEDURE

Epitaxial $(\text{GaAs})_{1-x}(\text{Si}_2)_x$ alloys with $0 < x < 0.53$ were grown on As-stabilized GaAs(001) substrates and $(\text{GaAs})_{1-x}(\text{Si}_2)_x/\text{GaAs}$ strained-layer superlattice buffer layers on GaAs(001) by a hybrid sputter-deposition-evaporation technique.⁶ The sputtering targets consisted of undoped single-crystal wafers of GaAs and Si. Excess As was provided by evaporation from an effusion cell. The total arsenic flux at the substrate was progressively decreased for the growth of alloys with higher Si contents. Film growth was carried out at a temperature of $(570 \pm 10)^\circ\text{C}$ and film thicknesses were typically 2–3 μm . Bulk alloy films with $x \leq 0.20$ were found to be defect-free as judged by a combination of plan-view transmission electron microscopy (TEM) and cross-sectional TEM while alloys with higher Si concentrations contained threading dislocations.⁶ Sample preparation for reflectance measurements consisted of rinsing in isopropyl alcohol.

Reflectance anisotropies were measured using a reflectance difference (RD) technique^{15–20} in which the difference in reflectivity is determined for linearly polarized light incident along the $[110]$ and $[1\bar{1}0]$ directions. Light from a Xe lamp is dispersed through a 0.25-m monochromator and intersects the sample, which is rotated at a frequency $f = 25$ Hz, at an angle of 5° from the $[001]$ normal. Reflected light is detected using an uv-enhanced photodiode whose output is fed into a lock-in amplifier tuned to a frequency of $2f$. The signal is processed by a microcomputer which stores the average reflectance $R = (R_{1\bar{1}0} + R_{110})/2$ along the two optical axes, the difference in reflectivity $\Delta R = R_{1\bar{1}0} - R_{110}$, and

$\Delta R/R$ at each photon energy. Al mirrors, rather than quartz lenses, were used to focus the incoming light onto the sample and the reflected light onto the photodiode in order to avoid chromatic effects. Further details concerning the optical system are given in Ref. 19.

The films were also examined using triple-crystal x-ray diffraction (XRD). The rotating Mo anode was typically operated at 35 kV and 60 mA and the monochromator and analyzer crystals were Ge(001). The ratios of the integrated intensities of the fundamental peaks (004, 008, etc.) to the superstructure peaks (002, 006, etc.) are related to the long-range order in the alloys.³

III. EXPERIMENTAL RESULTS

Typical high-resolution XRD patterns from alloy films with $x=0.20, 0.30, 0.37,$ and 0.53 are plotted in Fig. 1 over the range in diffraction angles corresponding to the (002) and (004) reflections. The superstructure (002) reflections due to the difference in average atomic scattering factors from the group-III and -V sublattices,¹³ are clearly seen near the corresponding GaAs substrate reflections in XRD patterns from the $x=0.20$ and 0.30 alloys. The (002) peak is barely resolvable in the $x=0.37$ pattern and is not observed at all in the pattern from the $x=0.53$ sample. These results indicate that the zincblende-to-diamond transition occurs near $x=0.37$.

Figure 2 shows normalized $\Delta R/R$ optical anisotropy spectra from a series of $(\text{GaAs})_{1-x}(\text{Si}_2)_x$ alloys with x ranging from 0 to 0.53. Measurements obtained from a

Si wafer, exhibiting no anisotropy, are also presented in Fig. 2 for reference. All points are raw data with no smoothing. The uppermost spectra from pure GaAs(001) exhibits well-defined structure at energies near critical points in the reduced Brillouin zone: $E_1, E_1+\Delta_1, E'_0,$ and E_2 .²¹ The oscillation with a maximum at E_1 (2.92 eV) and a minimum at $E_1+\Delta_1$ (3.15 eV) was shown previously to be due primarily to a bulk linear electro-optic effect.^{19,20} The more prominent structure occurs near the E'_0 point (4.5 eV). The physical origin of this feature, which has been observed previously,^{16,17} has been suggested to be due to a local surface field effect.²²⁻²⁵

The intensities of the optical anisotropy features in the alloy spectra decrease with increasing Si concentration. The optical structure is barely resolvable in the spectra from the film with $x=0.34$, while the spectra from the $x=0.53$ sample is featureless although the signal intensity still increases slightly with increasing energy. Figure 2 also shows that the spectral features around the prominent optical structure at 4.5 eV in GaAs shift to lower energies with increasing Si concentration. This is consistent with the fact that the corresponding E'_0 transition in Si occurs at 3.4 eV.²⁵

Before discussing the $(\text{GaAs})_{1-x}(\text{Si}_2)_x$ RD optical anisotropy measurements, we present the results of a further experiment carried out to probe the origin of the anisotropy effect in $A^{\text{III}}B^{\text{V}}$ (001) lattices. Figure 3 shows RD spectra from GaAs(001) (solid line) and GaAs(00 $\bar{1}$) (dashed line). Both spectra were obtained from the same

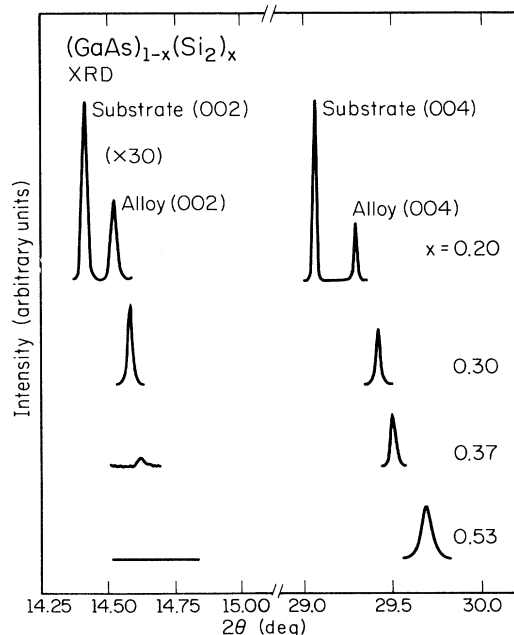


FIG. 1. High-resolution x-ray-diffraction patterns showing fundamental (004) and superstructure (002) reflections from epitaxial $(\text{GaAs})_{1-x}(\text{Si}_2)_x$ alloys with $x=0.20, 0.30, 0.37,$ and 0.53 . Diffraction peaks from a GaAs substrate are also shown.

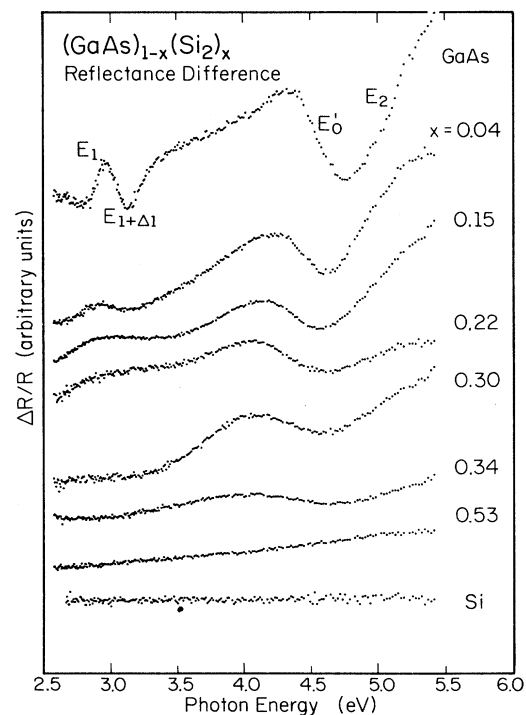


FIG. 2. Normalized $\Delta R/R$ optical anisotropy spectra from $(\text{GaAs})_{1-x}(\text{Si}_2)_x$ alloys.

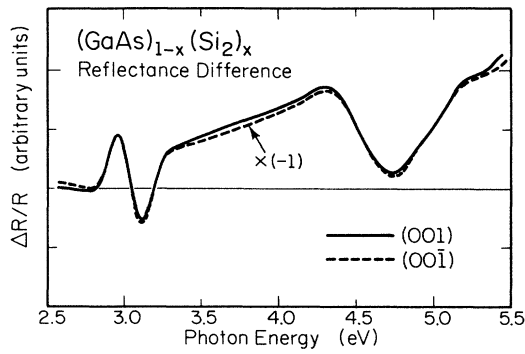


FIG. 3. $\Delta R/R$ optical anisotropy spectra from GaAs(001) (solid curve) and GaAs(00 $\bar{1}$) (dashed line, multiplied by -1) after a rotation of 180° about the $[110]$ axis.

GaAs wafer rotated 180° about the $[110]$ axis. The RD spectra are essentially identical in amplitude and differ only in sign (the dashed curve was multiplied by -1). The RD spectrum obtained from GaAs(00 $\bar{1}$) after a 180° rotation about the $[010]$ axis yields identical results, in amplitude *and* sign, as those from the initial GaAs(001) surface.

IV. DISCUSSION

Si(001), which has the same space lattice as GaAs(001), exhibits no optical anisotropy effect. This suggests that

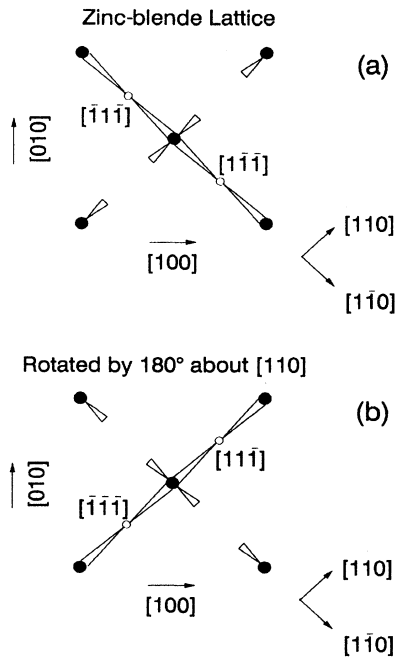


FIG. 4. Schematic diagram illustrating cation (solid circles) to anion (open circles) bond directions for (a) a (001)-oriented zinc-blende lattice and (b) a (00 $\bar{1}$)-oriented lattice obtained by rotating (a) by 180° about the $[110]$ direction.

the existence of an anisotropy in (001)-oriented zinc-blende samples requires well-ordered anion and cation sublattices. The presence of sublattices alone, however, does not lead to anisotropy. The results of the GaAs wafer rotation experiment described in Sec. III can be explained if we further assume that the air-exposed GaAs(001) and GaAs(00 $\bar{1}$) surfaces are preferentially Ga or As terminated rendering the upper few layers of the crystal anisotropic. In a zinc-blende lattice with a cation (anion) terminated (001) surface, the bond directions between a surface cation (anion) and the anion (cation) immediately below it are $[\bar{1}\bar{1}\bar{1}]$ and $[1\bar{1}\bar{1}]$ as shown in Fig. 4(a). Thus, incident light linearly polarized along $[110]$ has its electric-field vector \bar{E} orthogonal to the surface bond directions. However, light polarized along $[1\bar{1}0]$ has an \bar{E} component parallel to the bond directions. Rotating the GaAs(001) wafer 180° about either the $[100]$ or $[010]$ axes results in no change in the bond directions and hence leaves the sign of the RD signal invariant. However, a rotation of 180° about $[110]$, equivalent to a 90° rotation about $[001]$, transposes the cation-anion (anion-cation) bond directions to $[11\bar{1}]$ and $[\bar{1}\bar{1}\bar{1}]$ [see Fig. 4(b)], thus reversing the relationship of the \bar{E} vector with the incident light and changing the sign (but not the magnitude) of the RD spectrum as observed.

Consider now the RD results for the $(\text{GaAs})_{1-x}(\text{Si}_2)_x$ alloys. From the arguments given above, we expect that the degree of optical anisotropy should correlate directly

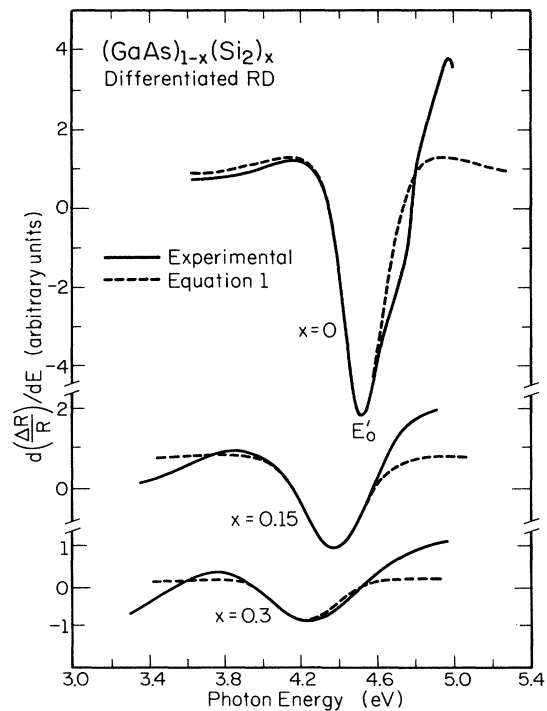


FIG. 5. Derivative $d(\Delta R/R)/dE$ optical anisotropy spectra from $(\text{GaAs})_{1-x}(\text{Si}_2)_x$ alloys with $x=0, 0.15,$ and 0.30 . The spectra are fitted using Eq. (1).

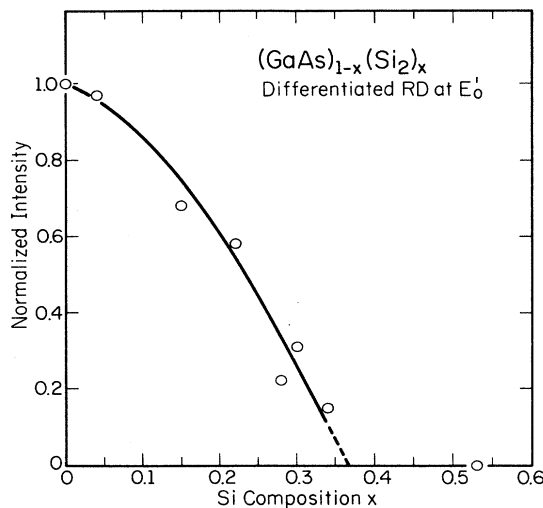


FIG. 6. Amplitude of the $d(\Delta R/R)/dE$ derivative spectra obtained from $(\text{GaAs})_{1-x}(\text{Si}_2)_x$ alloys as a function of the Si concentration x .

with the long-range order in the alloy. However, since the E_1 and $E_1 + \Delta_1$ features contain components due to a bulk linear electro-optic effect and hence depend upon the doping level and impurity type, we have chosen to concentrate our analysis on the spectral region near E'_0 where the electro-optic effect is relatively weak due to broadening and the anisotropy does not depend strongly on doping.^{19,20}

The magnitude of the anisotropic effect around the E'_0 point as a function of the Si concentration is more conveniently defined using derivative spectra. Typical results are shown in Fig. 5 in which the amplitude of the derivative peak decreases with increasing x and the peak broadens. In order to account for the broadening and obtain a quantitative measure of the $d(\Delta R/R)/dE$ peak amplitude, we have fit the peak line shapes with an ex-

pression of the form

$$\frac{d}{dE} \left[\frac{\Delta R}{R} \right] = A \frac{d}{dE} \left[\frac{E - E_p}{(E - E_p)^2 + \Gamma^2} \right], \quad (1)$$

where A is the amplitude of the derivative peak, E_p is the peak energy, and Γ is a broadening parameter. The energy dependence in Eq. (1) is commonly used to describe the real part of the dielectric function in reflectance-modulated spectra.²⁷ Equation (1) provides a good fit to all data in the present experiments and yields the correct $\Gamma_{15} - \Gamma_{25'}$, band gap for GaAs at room temperature, 4.5 eV.²¹

Figure 6 is a plot of the fitted amplitude of the anisotropy derivative spectra, normalized to that of GaAs, as a function of Si concentration. The amplitude, which is directly correlatable with the long-range order in the alloys, decreases monotonically with increasing x . The $(\text{GaAs})_{1-x}(\text{Si}_2)_x$ zinc-blende-to-diamond transition obtained from this analysis occurs near $x=0.37$ in agreement with the XRD results.

V. CONCLUSIONS

We have demonstrated that reflectance-difference spectroscopy can be used to determine long-range ordering, and in particular the zinc-blende-to-diamond transition, in $(A^{\text{III}}B^{\text{V}})_{1-x}(C_2^{\text{IV}})_x$ alloys. In addition, we have shown that the origin of the optical anisotropy near the E'_0 point in $A^{\text{III}}B^{\text{V}}(001)$ samples is primarily a surface effect due to the combination of preferential surface termination, well-defined cation and anion sublattices, and alternating bond directions as a function of depth.

ACKNOWLEDGMENTS

The authors gratefully acknowledge the financial support of the Secretaria de Educación Pública, Consejo Nacional de Ciencia y Tecnología, Organización de los Estados Americanos, and the Materials Science Division of the U.S. Department of Energy during the course of this research.

- ¹S. A. Barnett, M. A. Ray, A. Lastras, B. Kramer, J. E. Greene, P. M. Raccach, and L. L. Abels, *Electron. Lett.* **81**, 891 (1982).
- ²L. T. Romano, I. M. Robertson, J. E. Greene, and J. E. Sundgren, *Phys. Rev. B* **36**, 7523 (1987).
- ³K. C. Cadien, A. H. Eltoukhy, and J. E. Greene, *Vacuum* **31**, 253 (1981); *Appl. Phys. Lett.* **38**, 773 (1981).
- ⁴L. Romano, J. E. Sundgren, S. A. Barnett, and J. E. Greene, *Superlatt. Microstruct.* **2**, 233 (1986).
- ⁵S. I. Shah, J. E. Greene, L. K. Abels, Q. Yan, and P. M. Raccach, *J. Cryst. Growth* **83**, 3 (1987).
- ⁶D. H. Mei, Y.-W. Kim, D. Lubben, I. M. Robertson, and J. E. Greene, *Appl. Phys. Lett.* **55**, 2649 (1989).
- ⁷K. E. Newman, A. Lastras-Martínez, B. Kramer, S. A. Barnett, M. A. Ray, J. D. Dow, J. E. Greene, and P. M. Raccach, *Phys. Rev. Lett.* **50**, 1466 (1983).
- ⁸B. Kramer, G. Tomasch, M. Ray, J. E. Greene, L. Salvati, and T. L. Barr, *J. Vac. Sci. Technol. A* **6**, 1572 (1988).
- ⁹J. E. Greene, S. A. Barnett, K. C. Cadien, and M. A. Ray, *J.*

Cryst. Growth **56**, 389 (1982).

- ¹⁰T. N. Krabach, N. Wada, M. V. Klein, K. C. Cadien, and J. E. Greene, *Solid State Commun.* **45**, 895 (1983).
- ¹¹T. C. McGlenn, M. V. Klein, L. T. Romano, and J. E. Greene, *Phys. Rev. B* **38**, 3362 (1988).
- ¹²E. A. Stern, F. Ellis, K. Kim, L. Romano, S. I. Shah, and J. E. Greene, *Phys. Rev. Lett.* **54**, 905 (1985).
- ¹³S. I. Shah, B. Kramer, S. A. Barnett, and J. E. Greene, *J. Appl. Phys.* **59**, 1482 (1986).
- ¹⁴K. C. Cadien, B. C. Muddle, and J. E. Greene, *J. Appl. Phys.* **55**, 4177 (1984).
- ¹⁵D. E. Aspnes and A. A. Studna, *Phys. Rev. Lett.* **54**, 1956 (1985).
- ¹⁶D. E. Aspnes, *J. Vac. Sci. Technol. B* **3**, 1138 (1985).
- ¹⁷D. E. Aspnes, *J. Vac. Sci. Technol. B* **3**, 1498 (1985).
- ¹⁸D. E. Aspnes and A. A. Studna, *J. Vac. Sci. Technol. A* **5**, 546 (1987).
- ¹⁹S. E. Acosta-Ortiz and A. Lastras-Martínez, *Solid State Com-*

- mun. **64**, 809 (1987).
- ²⁰S. E. Acosta-Ortiz and A. Lastras-Martínez, *Phys. Rev. B* **40**, 1426 (1989).
- ²¹D. E. Aspnes and A. A. Studna, *Phys. Rev. B* **7**, 4605 (1973).
- ²²L. W. Mochan and R. G. Barrera, *J. Phys. (Paris) Colloq.* **45**, C5-207 (1984).
- ²³L. W. Mochán and R. G. Barrera, *Phys. Rev. Lett.* **55**, 1192 (1985).
- ²⁴L. W. Mochán (private communication).
- ²⁵D. Daunois and D. E. Aspnes, *Phys. Rev. B* **18**, 1824 (1978).
- ²⁶D. E. Aspnes, in *Handbook on Semiconductors Vol. 2*, edited by M. Balkanski (North-Holland, Amsterdam, 1980), p. 109.